Mechanically Linked Poly(ethylene terephthalate)

C. A. Fustin,[†,⊥] G. J. Clarkson,[‡] D. A. Leigh,[*,§] F. Van Hoof,[†] A. M. Jonas,[†] and C. Bailly[*,†]

Unité de Physique et de Chimie des Hauts Polymères, Université catholique de Louvain, Place Croix du Sud 1, B-1348 Louvain-la-Neuve, Belgium; Centre for Supramolecular and Macromolecular Chemistry, Department of Chemistry, University of Warwick, Gibbert Hill Road, Coventry CV4 7AL, United Kingdom; and School of Chemistry, University of Edinburgh, The King's Buildings, West Mains Road, Edinburgh EH9 3JJ, United Kingdom

Received July 14, 2004; Revised Manuscript Received August 13, 2004

ABSTRACT: The synthesis, by solid-state copolymerization, and properties of poly(ethylene terephthalate) (PET) copolymers containing various amounts of [2]catenane mechanical linkages are described. Polymers end-capped by the corresponding noninterlocked macrocycle as well as a copolymer with a rigid fluorene monomer unit were also prepared as reference systems. Size exclusion chromatography and ^{1}H NMR indicate that the catenane is quantitatively incorporated during synthesis but that a small fraction ring-opens to form noninterlocked macrocycles, incorporated as either chain ends or branching points. Catenanes induce a smaller increase in the glass transition temperature than the macrocycle at the same weight content. This is probably due to the suppression of interchain hydrogen bonds upon interlocking and points to a specific effect of the mechanical linkage on properties. The crystallization and melting temperatures of catenane copolymers are only slightly depressed compared to those of PET homopolymer, further demonstrating significant flexibility of the catenane rings. SAXS results show that the amorphous interlayer between lamellae increases with increasing catenane content at constant lamellar thickness, confirming that the uncrystallizable catenane units concentrate in the amorphous phase during solid-state polymerization.

Introduction

The incorporation of mechanically interlocked rings, i.e., catenanes, into a covalently bonded polymer is in principle an attractive strategy for the modification of conventional polymer properties.[1−14] If flexible (or switchable) catenane linkages are incorporated, the polymer chains should gain new degrees of freedom, significantly affecting the dynamics and conformation of the polymer backbone. This could, in turn, influence various solid-state, rheological, and solution properties. However, thus far very few examples of well-defined systems have been prepared in sufficient quantities for these issues to be experimentally addressed. We recently described[15] the synthesis of bisphenol A polycarbonate (PC) copolymers containing various amounts of a flexible benzylic amide [2]catenane incorporated by solid-state polymerization. This mechanically linked analogue of an important commercial polymer allowed for the detailed characterization of a well-understood system which unambiguously showed the influence of mechanical linkages on several important solution and solid-state properties. Catenane flexibility and mobility within the polymer chain were demonstrated by the limited effects of catenane incorporation on the glass transition temperature and the presence of a new mechanical transition below room temperature. However, PC is a somewhat rigid polymer, and it could be argued that these results do not constitute a severe test of catenane mobility within a polymer chain. Furthermore, because of the very slow crystallization of PC, it was not possible to assess the influence of the mechanical links on crystallization rate, a key property dependent upon chain flexibility. Here we describe the effects of incorporating mechanical linkages into a complementary commercial polymer, poly(ethylene terephthalate) (PET). PET has been commercially available since the 1950s and is arguably the most important engineering polymer in the world today, finding applications in fields as diverse as textile fibers, soft-drink bottles, food containers, and support film for magnetic recordings or photography, etc. The enhanced flexibility of PET over PC is demonstrated by its lower glass transition temperature (∼75 °C) and relatively fast crystallization rate. Although PET can be quenched from the melt, it readily recrystallizes upon heating.

The objective of this work was to assess the influence of catenane incorporation on the solid-state and melt properties of PET. We used a copolymerization method to introduce a [2]catenane similar to that used previously for PC.[15] In this way we were able to incorporate [2]catenane linkages into PET as 5−20 wt % (0.8−3 mol %) of repeat units. To build up our understanding of the role played by the mechanical bond, PET copolymers incorporating a rigid bulky comonomer 4,4′-(9-fluorenylidene)bis(2-phenoxyethanol) (10 wt %) as well as PET end-capped by the corresponding noninterlocked macrocycle (5−10 wt %) were prepared for property comparisons. The bis-functional [2]catenane[16−18] **1** used in this study was synthesized on a multigram scale without the need of chromatography. Catenane **1** contains two hydroxyethyloxyl groups and is thus suitable as a comonomer for the synthesis of PET copolymers. The rings can interact via intramolecular hydrogen bonds, and hence their mobility is partly restricted. In

† Université catholique de Louvain.
‡ University of Warwick.
§ University of Edinburgh.
⊥ Present address: Unité CMAT, Université catholique de Louvain, Place L. Pasteur 1, B-1348 Louvain-la-Neuve, Belgium.
* To whom correspondence may be addressed: bailly@poly.ucl.ac.be (fax +32-10-451593) or David.Leigh@ed.ac.uk (fax +44-131-6679085).

10.1021/ma048575u CCC: $27.50
Published on Web 09/23/2004

Scheme 1. Synthesis of Catenane 1 and of Macrocycle 2[a]

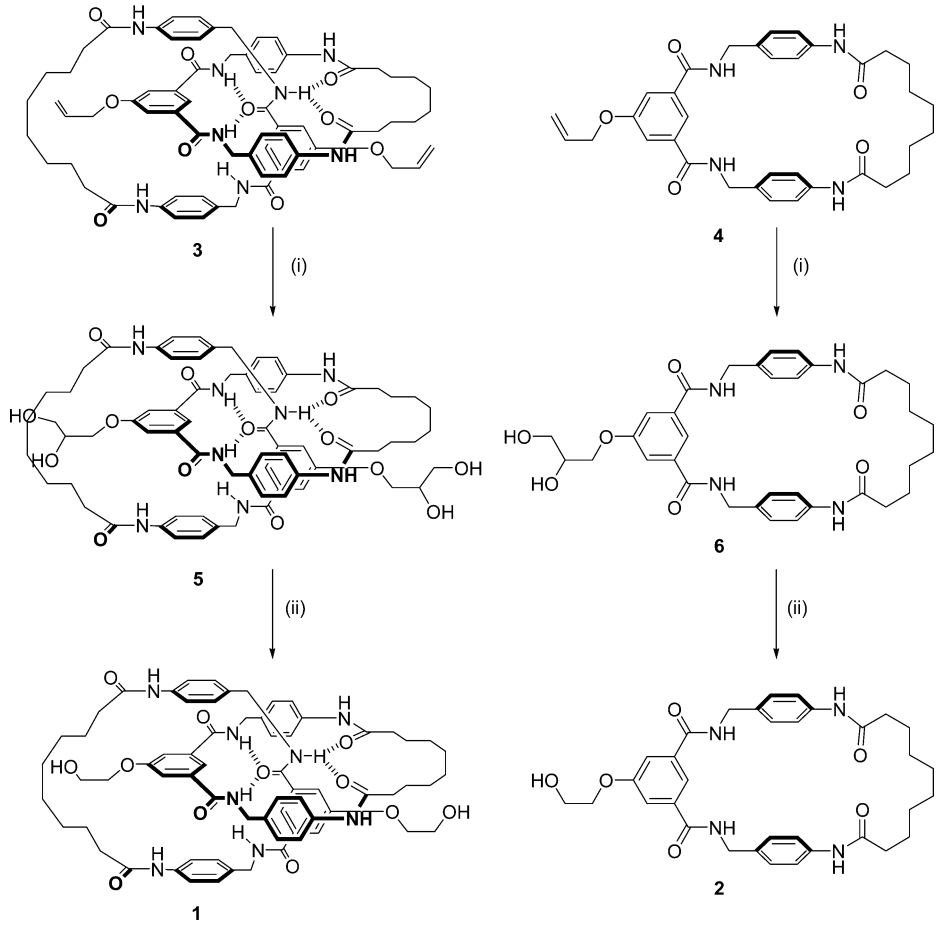

[a] (i) NMO, OsO_4, THF (catenane) or DMAc (macrocycle), 72% catenane; (ii) $NaIO_4$, $NaBH_4$, DMF/THF, 63% catenane.

Scheme 2. Synthesis of PET Prepolymer

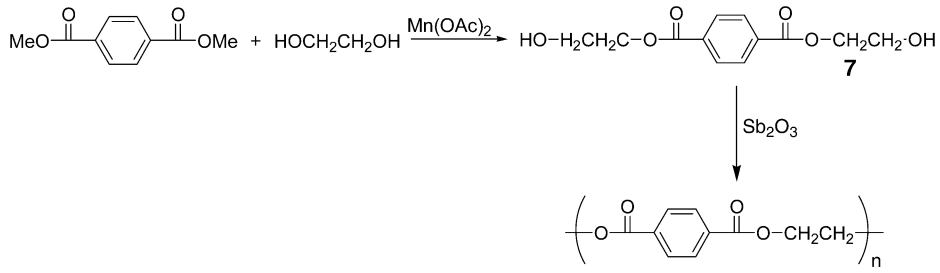

this respect, the PET catenane comonomer used in this study is significantly different from the one used for the polycarbonate copolymers reported previously.[15] In the latter case, the amide groups were methylated, which suppressed hydrogen bonding and enhanced rotational mobility. The comparison between these two examples should bring about new insights concerning the influence of ring mobility on copolymer properties. Here we focus on proving that the catenanes have been quantitatively incorporated into the polymer and on the discussion of some solid-state properties, especially crystallization.

Results and Discussion

Catenane Monomer Synthesis. The benzylic amide [2]catenane **1** and macrocycle **2** were prepared according to Scheme 1. Catenane **3**, the synthesis of which has already been described elsewhere,[15] was reacted with *N*-methylmorpholine-*N*-oxide (NMO) and osmium tetroxide to give the tertahydroxycatenane **5** in 72% yield. Catenane **5** was then converted into the bishydroxycatenane **1** (63% yield) by reaction with sodium periodate followed by sodium borohydride. Macrocycle **4**[15] was converted into macrocycle **2** following a similar procedure. Details of the synthesis are provided in the Experimental Section.

Polymer Synthesis. PET prepolymer was obtained in two steps as described in Scheme 2. Bis(2-hydroxyethyl) terephthalate (BHET) **7** was first synthesized from dimethyl terephthalate (DMT) and ethylene glycol with manganese acetate as catalyst following a modification of a reported procedure.[19] BHET was then polymerized by melt polycondensation with antimony trioxide as catalyst to yield low molecular weight PET. Size exclusion chromatography (SEC) was used to characterize the molecular weight distribution of the prepolymer (M_w = 13 kg/mol, M_n = 7.4 kg/mol). Differential scanning calorimetry (DSC) was performed on the amorphous prepolymer to yield a glass transition temperature of 72 °C and a melting point of 259 °C.

Scheme 3. Synthesis of PET Copolymers with (i) Catenane 1 and (iii) Fluorene 8 and of End-Capped Polymer with Macrocycle 2 (ii)

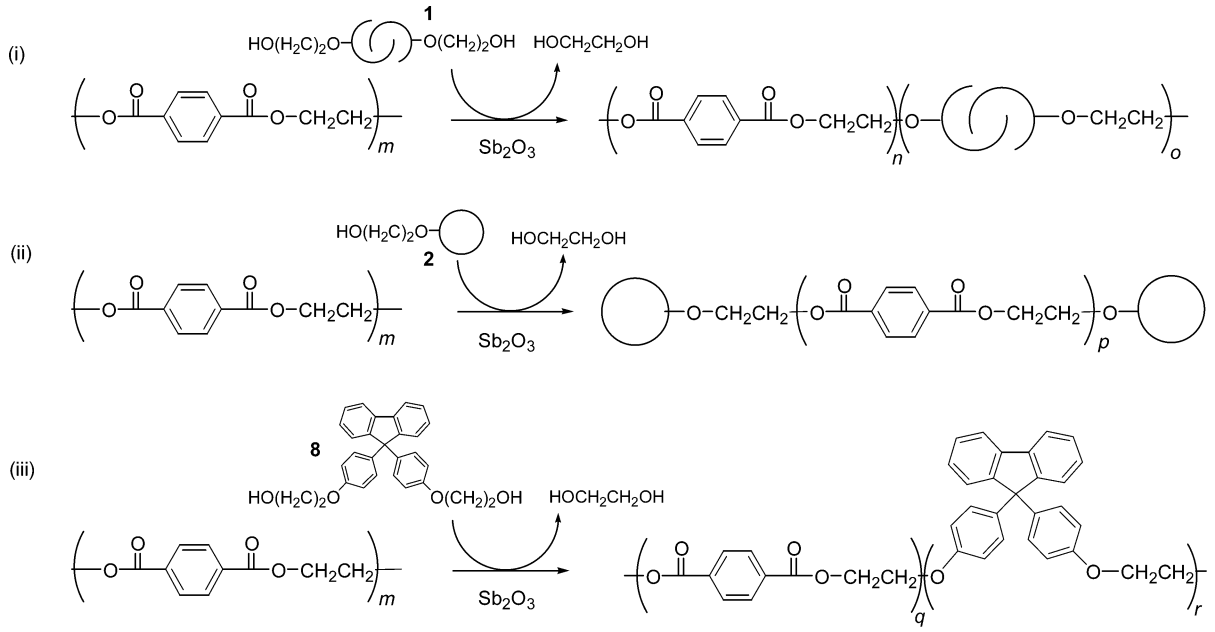

A 5, 10, or 20 wt % amount of catenane **1** or 5 or 10 wt % of macrocycle **2** (Scheme 3) and PET prepolymer were copolymerized by solid-state polymerization (SSP) after solution blending. The reaction was performed under vacuum (approximately 6×10^{-2} mbar) by applying an increasing temperature program from 160 to 215 °C for approximately 25 h total (details in Experimental Section). We confirmed that this program does not lead to loss of catenane monomer from the mixture by evaporation/sublimation. Since solid-state polymerization requires crystalline precursors,[20,21] the first step of the temperature program (160 °C) was dedicated to crystallize the blend. In this case, crystallinity of the blends offers an important advantage: upon crystallization, most defects—including catenane and chain ends—are rejected in the amorphous phase. Catenanes and chain ends are therefore in close proximity and can react together more easily. Furthermore, the reaction conditions are much milder than melt polycondensation, thus minimizing the chance of catenane degradation.

Quantitative Monomer Incorporation. SEC was used to determine whether catenanes have been quantitatively incorporated into PET. Samples coming out of SSP are highly crystalline and are often difficult to solubilize. Therefore, crystallinity was first eliminated by a quick heating−cooling cycle before dissolution in 1,1,1,3,3,3-hexafluoro-2-propanol (HFIP) and dilution with chloroform. Figure 1 shows SEC chromatograms of the PET prepolymer blend containing 20 wt % catenane **1** before and after SSP. The peak attributed to catenane monomer (around 21 min) has completely disappeared after polymerization. Since catenane could not escape from the reacting mixture by evaporation and since the total dissolved sample was injected in the SEC columns, all catenanes must have been incorporated into PET, and no free catenanes remain after SSP. A small shoulder is visible on the tail of the chromatogram at the low retention time side. This shoulder, observed for all three compositions, evidences some degree of heterogeneity in the copolymers. The exact origin of the observed shoulder is difficult to ascribe at this point.

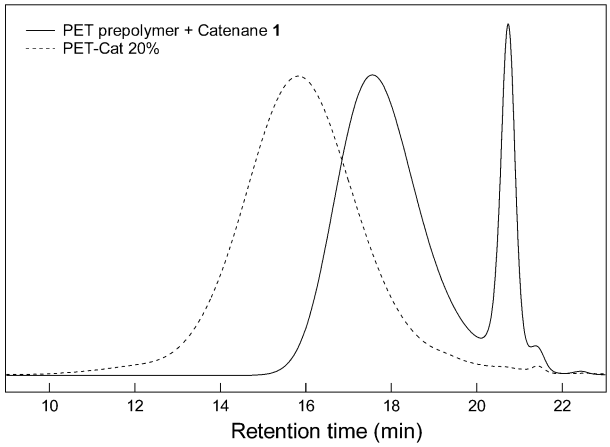

Figure 1. SEC traces in $CHCl_3$/HFIP of the blend of PET oligomers and catenane **1** (full line) and of the copolymer containing 20 wt % catenane **1** (dashed line).

However, the formation of branched chains certainly contributes to this shoulder since it was observed that a prolonged heating above T_m induces cross-linking. Catenane copolymers heated at 285 °C for 15 min are more difficult to solubilize and even form a gel for 20% catenane concentration. Moreover, an attempt to copolymerize catenane **1** and PET in the melt at 280 °C under vacuum, starting from the same blend as for SSP, yielded insoluble, highly cross-linked, polymer. Branching points can be produced by exchange reactions between catenane amide groups and PET ester functions. These reactions are indeed well-known in the case of melt blending of polyesters and polyamides.[22] The exchange reactions will open one macrocycle of the catenane to yield a branching point with three arms and a chain end-capped by the other macrocycle. During SSP those reactions are slower due to the lower temperature but can still occur. These results show that, despite the occurrence of some side reactions, the SSP copolymerization is a much milder and more efficient route than melt copolymerization. The small peak at the right-hand side of both chromatograms (and also present for PET

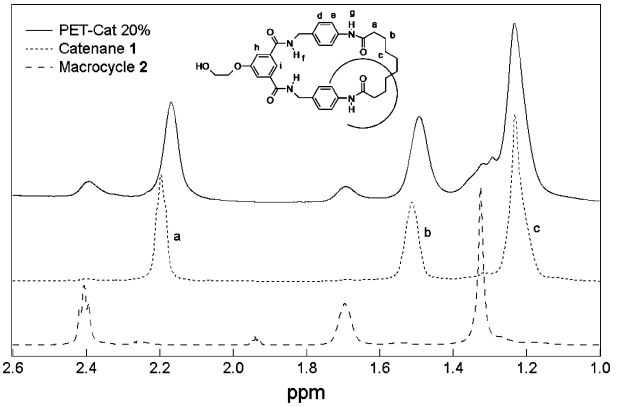

Figure 2. Aliphatic region of the ^{1}H NMR spectra of the copolymer containing 20 wt % catenane, of catenane **1**, and of macrocycle **2** recorded in $CDCl_3$/HFIP.

Table 1. PET Equivalent Molecular Weights of Copolymers Containing Various Amount of Catenane 1, Macrocycle 2, or Fluorene 8 Obtained by SEC in $CHCl_3$/HFIP

	M_n (kg/mol)	M_w (kg/mol)	PDI
PET	31	72	2.3
PET-Cat. 5%	25	67	2.7
PET-Cat. 10%	21	61	2.9
PET-Cat. 20%	17	52	3.0
PET-Mac 5%	19	51	2.7
PET-Mac 10%	13	40	3.1
PET-fluorene 10%	29	68	2.3

homopolymer) is associated with PET cyclic trimers.[23] Table 1 summarizes the molecular weight results, expressed in PET equivalents, for different copolymers. Compared to a PET homopolymer prepared under the same conditions, molecular weight decreases and polydispersity increases with increasing comonomer concentration. This is probably due to the side reactions mentioned above as well as to partial decomposition of the catenane into macrocycle (see below). This is not observed for the fluorene copolymer since in this case such side reactions cannot occur. As one could expect, the molecular weight of the macrocycle copolymers are lower than the PET homopolymer since the macrocycle is monofunctional and acts as chain stopper.

Solution ^{1}H NMR in $CDCl_3$/HFIP has been performed on the copolymers. The aliphatic proton region of the NMR spectrum of the copolymer containing 20 wt % catenane **1** is presented in Figure 2 together with the spectra of monomer catenane **1** and macrocycle **2**. This region's features are associated with protons of the alkyl chains of the catenane or of the macrocycle. The other aliphatic protons, i.e., the benzylic methylene groups and ethoxy groups, are situated at higher ppm but are hidden by the HFIP and PET ethoxy group peaks. The copolymer spectrum appears to be a superposition of the catenane and macrocycle spectra indicating that part of the catenane, 16% as determined by integration of the NMR peaks, has been decomposed into macrocycle during SSP. These macrocycles are not free since there is no corresponding peak on the chromatogram (Figure 1). Macrocycles can be produced by two parallel mechanisms: a thermal ring opening-ring closure mechanism, since it has been observed that a small amount of macrocycle is produced when catenane **1** is heated for a few hours at 215 °C under vacuum, and/or an amide-ester exchange reaction[22] between amides of the catenane and PET ester moieties. Macrocycles produced

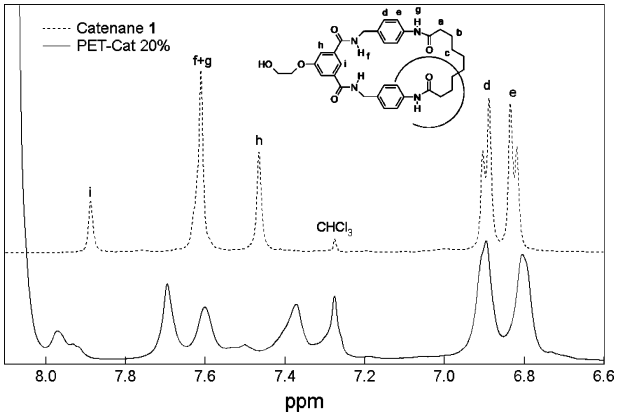

Figure 3. Aromatic region of the ^{1}H NMR spectra of the copolymer containing 20 wt % catenane and of catenane **1** recorded in $CDCl_3$/HFIP.

by the first mechanism can then react with PET to yield macrocycle end-capped chains. The existence of these side reactions was already hypothesized on the basis of the SEC results (see above). The amount of byproducts is, however, very small: 16% of 0.8 to 3 mol % starting catenane, making between 0.13 and 0.48 mol % of byproducts. This amounts, on average, to less than one branching point or macrocycle chain-end per chain, except in the case of the 20% copolymer. The percentage of catenane degraded into macrocycle is slightly higher for PET copolymers than for polycarbonate copolymers.[15] This could come from the fact that catenane **1** contains secondary amides instead of tertiary amides as is the case for the catenane incorporated into PC. Secondary amides are generally more reactive than tertiary amides due to less steric hindrance. The aromatic proton regions of the copolymer and catenane **1** NMR spectra are presented in Figure 3. The changes occurring in this region upon incorporation are much more pronounced than for the aliphatic region. The peaks situated on the catenane spectrum around 6.8 and 6.9 ppm, associated with protons of the para-substituted rings, do not change, but the three other peaks around 7.5, 7.6, and 7.9 ppm, linked to protons of the isophthaloyl rings and of the amide groups, are shifted to totally different positions. It is difficult to assign precisely the peaks in their new position because of their broad and unresolved features. However, the integration of this whole group of peaks compared to the integration of the two peaks at 6.8 and 6.9 ppm yields the correct intensity ratio considering the catenane structure. The changes occurring in the aromatic region of the NMR spectrum upon incorporation can be explained as follows. The catenane coconformation when incorporated into the PET is certainly different from the coconformation of a free catenane in solution, and hence the intramolecular hydrogen bond pattern may be somewhat different as well.[24,25] The isophthaloyl rings bear the functional tail by which the catenane is attached to PET and thus interact rather strongly with the polymer chain. This interaction, affecting the local environment of the isophthaloyl rings, could explain the different chemical shift observed for the protons of these rings compared to the catenane monomer. The peaks above 7.8 ppm on the copolymer spectrum are not linked to catenanes but are associated with the PET aromatic groups and chain ends. The NMR spectra of the other copolymers (not shown) are very similar to those shown

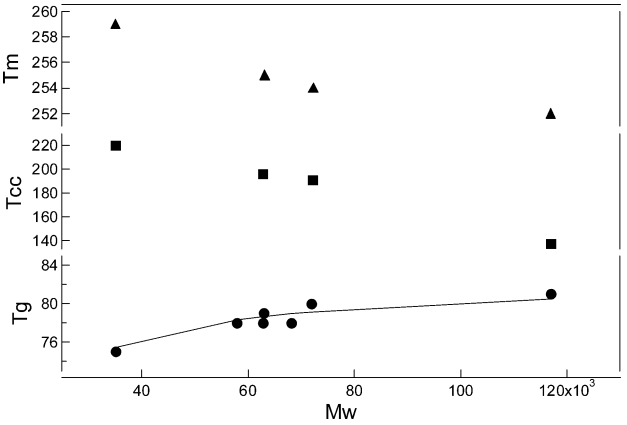

Figure 4. Dependence for pure PET of T_g (circle), T_{cc} (square), and T_m (triangle) according to molecular weight. The full line represents the Flory−Fox law determined on the basis of experimental data.

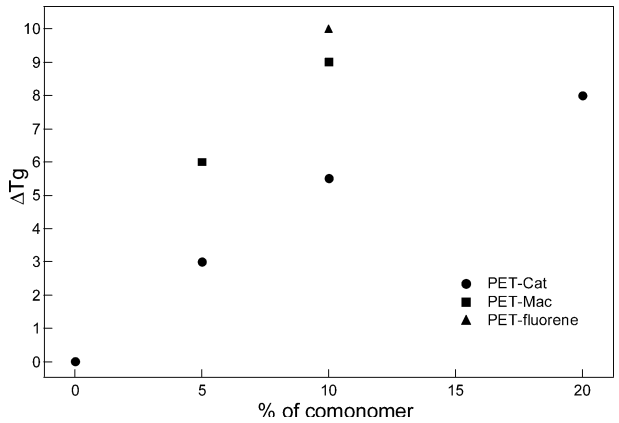

Figure 5. T_g variation with respect to pure PET of same molecular weight according to comonomer concentration (wt %).

in Figures 2 and 3, differing only by the intensity of the catenane peaks.

Solid-State Properties. It is known that the glass transition temperature (T_g), temperature of crystallization on cooling (T_{cc}), and melting temperatures (T_m) of PET vary with molar mass.[26] Since the molar masses of the different copolymers span a rather broad range, the evolution of T_g, T_{cc}, and T_m vs molecular weight has first been measured for PET homopolymers synthesized by the same method. The corresponding evolutions are presented in Figure 4. From the evolution of T_g vs molecular weight, the parameters of the Flory−Fox equation have been determined for the studied range of M_w:

$$T_g = 83 - 2.6 \times 10^2/M_w$$

for pure PET, with T_g in °C and M_w in kg/mol.

The data for the copolymers have then been compared to those predicted for pure PET at same molecular weight, and the differences have been plotted versus comonomer concentration. In this way, a clean dependence of the properties with respect to composition can be obtained. Figure 5 presents such a dependence for T_g, measured on amorphous quenched samples. The T_g of catenane copolymers and macrocycle end-capped polymers increases gradually with comonomer concentration, but the increase is higher for macrocycle end-capped polymers than for catenane copolymers. This

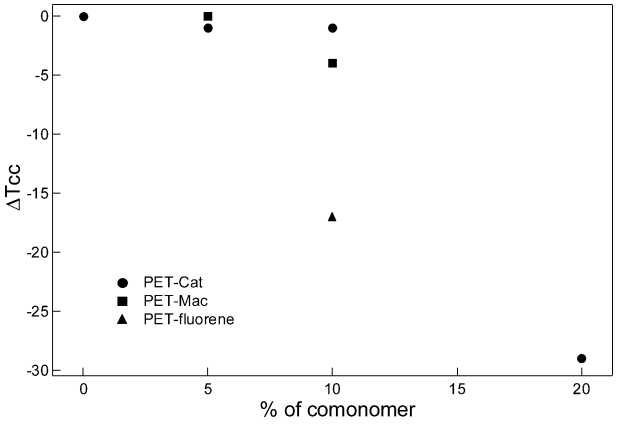

Figure 6. T_{cc} variation with respect to pure PET of same molecular weight according to comonomer concentration (wt %).

certainly comes from the formation of hydrogen bonds between the macrocycles and PET ester moieties or between macrocycles from different polymer chains. One macrocycle bears indeed four amide groups, and they cannot form intramolecular hydrogen bonds considering the macrocycle structure. The N−H moiety of the amides could thus form hydrogen bonds between polymer chains, and this will increase interchain interactions, decreasing overall chain mobility and thus increasing T_g. In the catenane, on the other hand, macrocycles are interlocked, and most of the amides are involved in intra-catenane hydrogen bonds, which partly restrict ring mobility,[24] but form fewer or no interchain hydrogen bonds. This induces a weaker T_g increase, resulting mainly from added in-chain rigidity. However, the T_g increase for the catenane copolymer is much smaller than is the case of a bulky, very rigid, comonomer such as fluorene **8**. At the same weight concentration, the molecular weight corrected T_g increase for the fluorene copolymer is twice as large as for the catenane, similar to the increase observed for the macrocycle end-capped polymers. This strongly suggests that, despite the intra-catenane hydrogen bonds, the catenane rings have still some degree of mobility since a completely rigid comonomer of comparable bulkiness induces a much larger T_g increase. The T_g behavior points therefore to a specific effect of the mechanical linkage on the solid-state properties. In a previous study on polycarbonate−catenane copolymers, it was observed that the macrocycle-containing polymers have a lower T_g than the catenane-containing copolymers at same level of incorporation. In the PC case, the dominant influence on T_g is the free volume increase associated with macrocycle chain ends, since hydrogen bonds are suppressed. The interlocking of the macrocycle rings to form catenanes compensates the free volume increase and thus raises T_g. In the present case, the dominant influence is hydrogen bonding. The interlocking of the catenane rings suppresses interchain hydrogen bonds and thus lowers T_g.

Evolution of the crystallization temperature on cooling (T_{cc}) vs comonomer concentration is presented in Figure 6. There is almost no change for 5% catenane or macrocycle, only a very small one for 10%, but a large decrease of about 30 °C for 20% catenane. These observations are confirmed by the evolution of the crystallization temperature on heating (T_{ch}). However, because of the difficulty in obtaining a reliable evolution of T_{ch} vs molecular weight in the case of pure PET, no

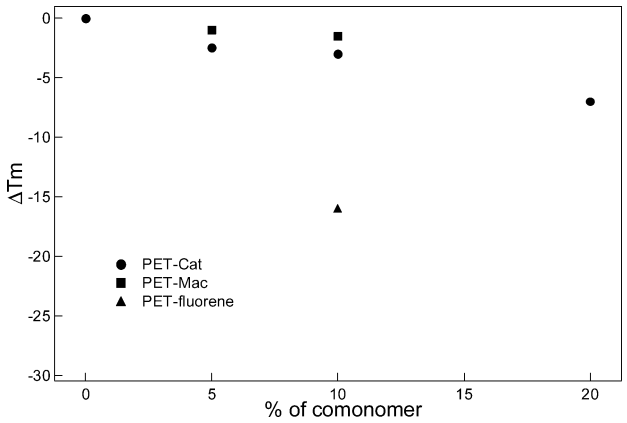

Figure 7. T_m variation with respect to pure PET of same molecular weight according to comonomer concentration (wt %).

values of ΔT_{ch} are given. The melting temperature follows the same evolution as T_{cc}: only a small decrease of T_m at low catenane concentration and a more important change for a concentration of 20 wt % (Figure 7). Surprisingly, the crystallization rate of the copolymers decreases only slightly when catenane concentration increases up to 10 wt %. It is important to notice that for a given concentration the decrease in T_{cc} is much larger for the copolymer containing the fluorene **8**. The catenane has thus little effect on chain mobility and on the crystallization of PET compared to very rigid comonomer, showing once again a certain degree of flexibility of the catenane rings. It is more difficult to interpret the changes observed for T_m and T_{cc} for the 20% catenane copolymer because of their uncertain origin. SEC results (see above) indeed suggest that this copolymer contains branched and/or cross-linked chains. Therefore, these results will not be further discussed. A comparison with results from the literature further confirms the surprisingly small influence of catenanes on the crystallization properties of PET. Usually, the incorporation of small amount (up to 10 mol %) of comonomers such as 1,4-cyclohexanedimethanol, isophthalic acid, 2,2-butyl-ethyl-1,3-propanediol, etc., decreases T_{cc} and T_m by several degrees.[27] For example, the incorporation in PET of 2.5 mol % phthalate, 1,8-naphthalenedicarboxylate, or 1,8-anthracenedicarboxylate induces a decrease of T_m between 4 and 9 deg and a decrease of T_{cc} between 18 and 24 deg, depending on the comonomer, much more than what we have observed for catenanes.[28]

The enthalpy of fusion (ΔH_m) of the copolymers has been measured by DSC during the first heating. Highly crystalline samples coming directly from SSP, and amorphous samples prepared by quenching in cold water have both been measured and compared to a PET homopolymer prepared also by SSP with the same temperature program. The crystallinity of the samples has been calculated on the basis of an enthalpy of fusion of 135.8 J/g for 100% crystalline PET homopolymer.[29] The results are reported in Table 2. The measured crystallinity of SSP samples is of course higher than the crystallinity measured on quenched/crystallized samples. SSP samples have indeed been annealed much longer at high temperature. Table 2 indicates that crystallinity of catenane and fluorene copolymers, up to 10% comonomer, is roughly equal to that of PET homopolymer. For the quenched copolymer containing 10% fluorene **8**, crystallinity is lower because of the slower crystallization kinetics, T_{ch} (167 °C) being indeed rather close to T_m (239 °C) for this copolymer. It is again interesting to compare the behavior of PET copolymers to the PC copolymers previously reported. In the latter case, we have observed a decrease of the absolute crystallinity after SSP with comonomer concentration but a constant "corrected" crystallinity, in the sense that the crystallinity of the crystallizable fraction remains constant.[30] These observations were consistent with the SSP process.[20,31] The resulting copolymers indeed consist of PC homopolymer blocks, the crystallizable fraction, and of random PC−catenane copolymer blocks, which are unable to crystallize. When the catenane concentration increases, the global amount of amorphous phase and the local catenane concentration in the amorphous phase increase, but the quality of the crystalline phase is unaffected. In the case of PET copolymers, although there is an indication that the absolute crystallinity is constant up to 10% comonomer, the differences with respect to constant "corrected" crystallinity are rather small (order of 6 J/g) and of the order of the experimental error. Therefore, the hypothesis of a constant "corrected" crystallinity remains consistent with the data. The results of the 20% catenane copolymer will not be discussed for the same reasons as discussed above (branching). Crystallinity of macrocycle end-capped polymers is higher than for the catenane copolymers and even higher than for the PET homopolymer. This is due to the much lower molecular weight of these polymers which tends to increase the crystallinity.

Table 2. Enthalpy of Fusion and Crystallinity Obtained on the First Heating DSC Trace Starting from Samples Coming Directly from the SSP and from Amorphous Samples Prepared by Quenching

	SSP		quenched	
	ΔH_m (J/g)	crystallinity (%)	ΔH_m (J/g)	crystallinity (%)
PET	60	44	36	26
PET-Cat. 5%	61	45	32	24
PET-Cat. 10%	61	45	32	24
PET-Cat. 20%	53	39	27	20
PET-Mac 5%	62	46	45	33
PET-Mac 10%	72	53	44	32
PET-fluorene 10%	58	43	24	18

SAXS measurements were performed on the copolymers after isothermal crystallization from the amorphous state at 160 °C for 15 min and then at 200 °C for 60 min to erase previous thermal history. Since it is known for PET that the long period and the thickness of amorphous interlamellar regions depend on the molar mass,[32] a PET homopolymer with a molecular weight (M_w = 63 kg/mol) close to the one of the 10% catenane copolymer was chosen as reference. Figure 8 presents the Lorentz-corrected scattering data vs momentum transfer q for the melted and recrystallized samples, together with their normalized Fourier transform (correlation function) and the opposite of the second derivative of the Fourier transforms (interface distribution functions). The Fourier transforms and their second derivatives allow us to estimate with precision the lamellar thickness and the long period of PET samples, as detailed elsewhere.[33] The incorporation of the catenane in the PET chain after SSP is clearly demonstrated by the SAXS data recorded after isothermal crystallization. Such conditions should lead to crystals of identical thickness L_c, according to standard crystallization theory, since the melting temperatures of the

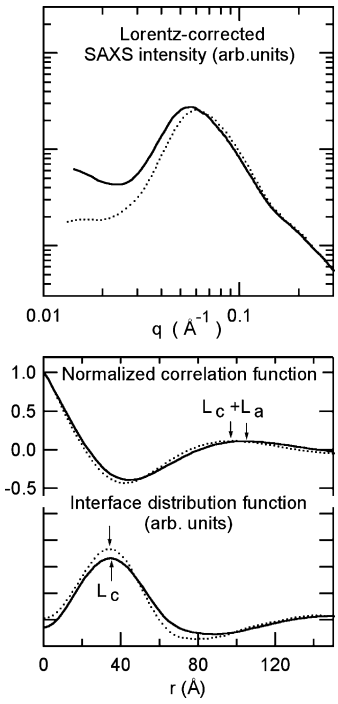

Figure 8. (top) Lorentz-corrected small-angle X-ray scattering of the samples of this study. (bottom) Normalized correlation function and interface distribution function computed from the SAXS. Dotted lines: PET homopolymer; continuous lines: PET-Cat. 10%. The samples were crystallized from the amorphous state at 160 °C for 15 min and then at 200 °C for 60 min to erase previous thermal history. The morphological parameters (estimates for the crystal thickness L_c and for thickness of amorphous interlamellar regions L_a) are indicated in the lower figure.[33]

two samples are close (255 °C for the PET homopolymer and 253 °C for the copolymer containing 10 wt % catenane).[34] This is confirmed by the examination of the locations of the first maximum of the interface distribution functions, which are a good estimates for L_c.[33] Values of 3.4 and 3.5 nm are found for PET homopolymer and the copolymer containing 10 wt % catenane, respectively. In contrast, the long period, which is properly estimated by the location of the first broad maximum in the correlation functions,[33] is significantly different for the two samples, since it increases from 9.7 to 10.5 nm upon incorporation of the catenane moieties. This may only be due to thicker interlamellar amorphous regions in the copolymers (L_a), corresponding to the accumulation of catenane-rich segments of the chains in these regions. These results are consistent with a constant "corrected" crystallinity as discussed above and are in complete agreement with a model of chain architecture consisting of catenane links interspersed among regular PET sequences.

Conclusion

The synthesis of PET copolymers containing various amounts of a benzylic amide [2]catenane and of polymers end-capped with the corresponding macrocycle has been achieved by solid-state copolymerization. During this process, catenane incorporation into the polymer is quantitative, but a small fraction of the catenane decomposes, yielding macrocycles, incorporated into PET as chain ends and/or branching points. If melt copolymerization is used, an insoluble polymer is obtained, confirming the versatility and usefulness of the solid-state process. The glass transition temperature of the PET−catenane copolymers increases with comonomer concentration but less than for macrocycle end-capped polymers. This difference is attributed to a specific effect of the catenane mechanical linkage (probably intra- vs intermolecular hydrogen bonding). The effect is opposite to that observed for PC−non-hydrogen-bonding catenane copolymers described previously, where free volume effects dominate and therefore macrocycles tend to reduce T_g. Moreover, for the same comonomer concentration, the T_g of a catenane-containing PET copolymer is well below the T_g of a copolymer containing a bulky and rigid comonomer at the same weight content. This observation suggests a significant relative internal mobility/flexibility of the catenane rings. Up to 10 wt % incorporation, the catenane has only a small influence on the crystallization properties of the PET copolymers, indicating once more the relative flexibility of the catenane rings. SAXS results indicate that the amorphous interlayer between crystalline lamellae grows thicker with increasing catenane comonomer content while the lamellar thickness remains constant. This in turn is consistent with a model previously observed for PC−catenane copolymers[15] where the uncrystallizable catenane units concentrate in the interlamellar amorphous phase during the solid-state process.

Experimental Section

Measurements. Size exclusion chromatography experiments were carried out on a Gilson system equipped with a Waters 484 UV tunable absorbance detector and two mixed bed HFIPgel columns from Polymer Laboratories. Universal calibration using polystyrene standards was performed. The chloroform/1,1,1,3,3,3-hexafluoro-2-propanol (HFIP) 98/2 mixture was used as solvent, and the flow rate was set to 0.8 mL/min. Mark−Houwink coefficients of pure poly(ethylene terephthalate)[23] were used for all copolymers, thus giving PET equivalent molecular weights. Before solubilization all SSP samples were dried under vacuum at 50 °C for 24 h and then heated to 280 °C for 1 min under dry nitrogen and quickly cooled to room temperature. Thermal analyses were performed on a Perkin-Elmer DSC 7, working with a heating rate of 10 °C/min. Before measurements, samples were dried under vacuum at 50 °C for 12 h. When amorphous samples were needed, the following procedure was applied to erase previous thermal history. Samples were dried in a vacuum at 50 °C for 24 h, then heated in a DSC pan to 280 °C for 2 min under a nitrogen atmosphere, and then quickly cooled by dipping the DSC pan in cold water to obtain amorphous samples. Samples were dried again under vacuum at 50 °C for 12 h just before the analysis. ^{1}H NMR spectra were recorded at room temperature on a Bruker Advance 500 MHz spectrometer, using deuterated chloroform/HFIP 85/15 mixture as solvent and as internal standard or on a Bruker Avance 400 MHz spectrometer using other solvents. Before solubilization all samples were dried under vacuum at 50 °C for 24 h. SAXS measurements were conducted in a Kratky camera (Anton-Paar KKK) using a Braun OED 50M proportional position-sensitive detector and Ni-filtered Cu Kα radiation form a copper anode generator operated at 40 kV/300 mA. They were performed on polymer powders encapsulated in glass capillaries of 2 mm diameter at room temperature and under primary vacuum. Acquisition data were spline-smoothed, corrected for parasitic scattering, desmeared, background-subtracted, and Lorentz-corrected, as described elsewhere.[35]

Solvents and Reagents. All solvents used were commercial HPLC grade. All other chemicals were purchased from Aldrich or Acros and used as received.

Synthesis. *Catenane **1***. The bis-allyloxycatenane **3** (0.5 g, 0.4 mmol), the synthesis of which has already been described

elsewhere,[15] was dissolved in the minimum of dimethylformamide (5 mL) and diluted with THF (20 mL). To the rapidly stirred solution was added a solution of *N*-methylmorpholine-*N*-oxide (50% in water, 0.5 mL, 0.6 g, 2 mmol). Osmium tetroxide in *tert*-butanol (0.5 mL, 2.5 wt %, catalytic) was added and the solution stirred until thin-layer chromatography (CH_2Cl_2/DMAc/MeOH (8:1:1), product rf 0.1) showed total consumption of starting material. The reaction mixture was then poured into an excess of rapidly stirred diethyl ether. The precipitate was filtered off and then recrystallized from 2-propanol/water to give tiny white cubes of tetrahydroxycatenane **5** (0.38 g, 72%); mp 216−219 °C, *m*/*z* 1261 $(M + H)^+$. ^{1}H NMR (400 MHz, d_6-DMSO) δ: 9.67 (4H, br s, NH), 8.40 (4H, br t, $J = 5.5$ Hz, NH), 7.70 (2H, s, ArH), 7.45 (4H, br s, ArH), 7.32 (8H, d, $J = 8.0$ Hz, ArH), 6.94 (8H, d, $J = 8.0$ Hz, ArH), 5.03 (2H, d, $J = 5.5$ Hz, OH), 4.72(2H, t, $J = 5.5$ Hz, OH), 4.10 (8H, br m, ArCH_2N) and CH_2CHOHCH_2), 3.80 (4H, br m, CH_2OH), 3.48 (4H, m, CH_2OAr), 2.13 (8H, br s, $COCH_2$), 1.30 (8H, br s, $COCH_2CH_2$) and 0.77 (16H, br s, CH_2).

The tetrahydroxycatenane **5** (0.5 g, 0.4 mmol) was dissolved in a mixture of dimethylformamide (5 mL) and THF (20 mL). To this stirred mixture was added an aqueous solution of sodium periodate (0.2 g, 0.9 mmol in 2 mL of water). The reaction was monitored by thin-layer chromatography (CH_2Cl_2/MeOH/DMAc: 7:1.5:1.5) until the starting material was consumed, and then sodium borohydride (50 mg) was added in small portions. The mixture was stirred for an hour and then filtered through a small pad of Celite, and the solvent was removed by evaporation under reduced pressure. The thick oil was purified twice by recrystallization from dimethylformamide/water to give the bis-hydroxycatenane **1** as tiny white needles (0.3 g, 63%); mp 248−250 °C, *m*/*z* 1201 $(M + H)^+$. $C_{68}H_{80}O_{12}N_8$ requires C, 67.98; H, 6.71; N, 9.33%. Found: C, 67.4; H, 6.8; N, 9.4%. ^{1}H NMR (400 MHz, d_6-DMSO) δ: 9.70 (4H, br s, NH), 8.37 (4H, br t, $J = 5.5$ Hz, NH), 7.72 (2H, br s, ArH), 7.45 (4H, br s, ArH), 7.34 (8H, d, $J = 8.0$ Hz, ArH), 6.94 (8H, d, $J = 8.0$ Hz, ArH), 4.93 (2H, t, $J = 5.5$ Hz, OH), 4.11 (8H, br s, ArCH_2), 3.94 (4H, br m, ArOCH_2CH_2OH), 3.73 (4H, br q, $J = 5.5$ Hz, ArOCH_2CH_2OH), 2.14 (8H, br s, $COCH_2$), 1.30 (8H, br s, $COCH_2CH_2$) and 0.81 (16H, br s, CH_2). ^{13}C NMR (100 MHz, d_6-DMSO) δ: 175.5, 170.0, 162.6, 142.2, 140.3, 136.6, 132.3, 122.8, 121.8, 120.1, 73.9, 63.5, 47.2, 40.1, 33.2, 32.1, and 29.3. FT-IR (KBr): 3320, 2935, 1645, 1607, 1540, 1520, 1415, 1310, and 1255 cm^{-1}.

*Macrocycle **2***. To a stirred solution of macrocycle **4** (1.5 g, 2.5 mmol), the synthesis of which has already been described elsewhere,[15] in dimethylacetamide (20 mL) at room temperature was added *N*-methylmorpholine-*N*-oxide monohydrate (95%, 0.37 g, 2.7 mmol) dissolved in dimethylacetamide (10 mL). OsO_4 (2.5 wt % solution in *tert*-butanol, 0.1 mL, catalytic) was added, and the solution stirred until thin-layer chromatography (CH_2Cl_2/MeOH/DMF (10:1:1), product rf 0.15) showed total consumption of starting material. The reaction mixture was then poured into an excess of rapidly stirred diethyl ether. The precipitate was filtered off and used without further purification. The tetrahydroxy macrocycle **6** was then dissolve in dimethylformamide (15 mL) and diluted with THF (10 mL). Sodium periodate (0.53 g, 2.5 mmol) was added in one portion to the stirred mixture. The reaction was monitored by thin-layer chromatography (CH_2Cl_2/DMAc/MeOH (10:1:1), product rf 0.6) until the material was consumed, and then sodium borohydride (100 mg, excess) was added in small portions and the mixture stirred for an hour. The mixture was then filtered through a small pad of Celite, and the solvent was removed to a small volume. This was then added to a rapidly stirred excess of water. The precipitate was filtered and recrystallized from DMF/water as small white cubes of macrocycle **2**; mp > 310 °C, *m*/*z* 601 $(M + H)^+$. $C_{34}H_{40}O_6N_4$ requires C, 67.98; H, 6.71; N, 9.33%. Found: C, 67.6; H, 6.8; N, 9.5%. ^{1}H NMR (400 MHz, d_6-DMSO) δ: 9.81 (2H, s, NH), 8.76 (2H, br t, $J = 5.4$ Hz, NH), 7.69 (1H, s, ArH), 7.51 (4H, d, $J = 8.4$ Hz, ArH), 7.48 (2H, br s, ArH), 7.24 (4H, d, $J = 8.4$ Hz, ArH), 4.94 (1H, t, $J = 5.5$ Hz, OH), 4.38 (4H, d, $J = 5.4$ Hz, ArCH_2), 4.11 (2H, t, $J = 5.0$ Hz, CH_2CH_2OH), 3.77 (2H, br q, $J = 5.0$ Hz, CH_2CH_2-OH), 2.29 (4H, br t, $J = 6.4$ Hz, $COCH_2CH_2$), 1.57 (4H, br m, $COCH_2CH_2$), and 1.24 (8H, br s, CH_2). ^{13}C NMR (100 MHz, d_6-DMSO) δ: 171.5, 166.1, 160.0,138.6, 136.7, 133.9, 128.8, 119.3, 118.2, 116.3, 70.3, 59.8, 43.1, 36.3, 29.4, 28.4, and 25.5.

PET Prepolymer. A three-necked round-bottom flask was charged with dimethyl terephthalate (194 g, 1 mol) and ethylene glycol (620 g, 10 mol), and manganese acetate (122.5 mg, 5×10^{-4} mol) was added as transesterification catalyst. A light nitrogen flux was applied, and the mixture was progressively heated to 200 °C. Stirring was switched on upon melting of dimethyl terephthalate (140 °C). The methanol produced by the transesterification was distilled off. Reaction was stopped when the production of methanol stopped. The mixture of prepolymer and ethylene glycol was poured in a crystallizing dish and allowed to cool. One liter of cold water was added in the crystallizing dish, and the mixture was filtered to separate the prepolymer from water and ethylene glycol. The prepolymer was dissolved in boiling water and filtered to separate BHET **7**, which is soluble in boiling water, from higher PET oligomers. The solution of BHET was then placed at 4 °C overnight to allow its recrystallization. The purification step was repeated twice.

A glass reactor was charged with BHET **7** (60 g, 0.24 mol), and antimony trioxide (18 mg, 6.2×10^{-5} mol) was added as transesterification catalyst. Vacuum (0.2 mbar) was applied, and the temperature was slowly (in 20 min) raised to 285 °C. Stirring was switched on when the temperature reached 200 °C, and the speed was set to 60 rpm. Reaction was stopped after 45 min. The system was then returned to atmospheric pressure, and the glass reactor was quickly removed from the oven and immersed in water to quickly cool PET.

Copolymer. Copolymerization was performed on batches of 300 mg. PET and catenane **1** (5, 10, and 20 wt %) or macrocycle **2** (5 and 10 wt %) or 4,4′-(9-fluorenylidene)bis(2-phenoxyethanol) **8** (10 wt %) were dissolved in 5 mL of HFIP. Solvent was evaporated under vacuum while stirring the solution, and the resulting powder was dried under vacuum for 12 h at 50 °C. After this step, the sample is already partially crystallized. The blend was ground to obtain a finely divided powder. Solid-state polymerization was performed under vacuum (6×10^{-2} mbar) applying the following temperature program: (i) room temperature for 30 min; (ii) 160 °C for 1 h; (iii) 190 °C for 1 h; (iv) 200 °C for 2 h; (v) 205 °C for 1 h; (vi) 210 °C for 18 h; (vii) 215 °C for 2 h. Heating was ensured by a salt bath enabling a temperature control within 2 °C.

Acknowledgment. This work has been supported by the European Community, TMR Contract No. HPRN-CT-2000-00024 (MIPA Network). D.A.L. is an EPSRC Advanced Research Fellow (Grant AF/982324). C.A.F. gratefully acknowledges support from UCL through an FSR grant.

References and Notes

(1) Raymo, F. M.; Stoddart, J. F. *Chem. Rev.* **1999**, *99*, 1643−1663.

(2) Geerts, Y. In *Molecular Catenanes, Rotaxanes and Knots*; Sauvage, J. P., Dietrich-Buchecker, C., Eds.; Wiley-VCH: Weinheim, 1999; pp 247−276.

(3) Clarkson, G. J.; Leigh, D. A. In *Emerging Themes in Polymer Science*; Ryan, A. J., Ed.; Royal Society of Chemistry: Cambridge, 2001; pp 299−306.

(4) For discussions of the effects on properties in polyrotaxanes where the mechanical linkage does not interrupt the covalent backbone of the polymer, see ref 1 and Gong, C. G.; Gibson, H. W. *Curr. Opin. Solid State Mater. Sci.* **1997**, *2*, 647−652. For daisy-chain-type polyrotaxanes and polypseudorotaxanes which do have rotaxane mechanical linkages in the polymer backbone see: (a) Gibson, H. W.; Yamaguchi, N.; Hamilton, L.; Jones, J. W. *J. Am. Chem. Soc.* **2002**, *124*, 4653−4665. (b) Cantrill, S. J.; Youn, G. J.; Stoddart, J. F.; Williams, D. J. *J. Org. Chem.* **2001**, *66*, 6857−6872. (c) Hoshino, T.; Miyauchi, M.; Kawaguchi, Y.; Yamaguchi, H.; Harada, A. *J. Am. Chem. Soc.* **2000**, *122*, 9876−9877. (d) Rowan, S. J.; Cantrill, S. J.; Stoddart, J. F.; White, A. J. P.; Williams, D. J. *Org. Lett.* **2000**, *2*, 759−762. (e) Gibson, H. W.; Hamilton,

L. M.; Yamaguchi, N. *Polym. Adv. Technol.* **2000**, *11*, 791−797. (f) Yamaguchi, N.; Gibson, H. W. *Angew. Chem., Int. Ed.* **1999**, *38*, 143−147. (g) Yamaguchi, N.; Hamilton, L. M.; Gibson, H. W. *Angew. Chem., Int. Ed.* **1998**, *37*, 3275−3279.
(5) Amabilino, D. B.; Ashton, P. R.; Reder, A. S.; Spencer, N.; Stoddart, J. F. *Angew. Chem., Int. Ed. Engl.* **1994**, *33*, 1286−1290.
(6) Geerts, Y.; Muscat, D.; Müllen, K. *Macromol. Chem. Phys.* **1995**, *196*, 3425−3435.
(7) Weidmann, J. L.; Kern, J. M.; Sauvage, J. P.; Geerts, Y.; Muscat, D.; Müllen, K. *Chem. Commun.* **1996**, 1243−1244.
(8) Muscat, D.; Witte, A.; Köhler, W.; Müllen, K.; Geerts, Y. *Macromol. Rapid Commun.* **1997**, *18*, 233−241.
(9) Hamers, C.; Raymo, F. M.; Stoddart, J. F. *Eur. J. Org. Chem.* **1945**, *10*, 2109−2117.
(10) Menzer, S.; White, A. J. P.; Williams, D. J.; Belohradsky, M.; Hamers, C.; Raymo, F. M.; Shipway, A. N.; Stoddart, J. F. *Macromolecules* **1998**, *31*, 295−307.
(11) Shimada, S.; Ishiwara, K.; Tamaoki, N. *Acta Chem. Scand.* **1998**, *52*, 374−376.
(12) Hamers, C.; Kocian, O.; Raymo, F. M.; Stoddart, J. F. *Adv. Mater.* **1998**, *10*, 1366−1369.
(13) Weidmann, J. L.; Kern, J. M.; Sauvage, J. P.; Muscat, D.; Mullins, S.; Köhler, W.; Rosenauer, C.; Räder, H. J.; Martin, K.; Geerts, Y. *Chem.—Eur. J.* **1999**, *5*, 1841−1851.
(14) Muscat, D.; Köhler, W.; Räder, H. J.; Martin, K.; Mullins, S.; Müller, B.; Müllen, K.; Geerts, Y. *Macromolecules* **1999**, *32*, 1737−1745.
(15) Fustin, C. A.; Bailly, C.; Clarkson, G. J.; De Groote, P.; Galow, T. H.; Leigh, D. A.; Robertson, D.; Slawin, A. M. Z.; Wong, J. K. Y. *J. Am. Chem. Soc.* **2003**, *125*, 2200−2207.
(16) Johnston, A. G.; Leigh, D. A.; Pritchard, R. J.; Deegan, M. D. *Angew. Chem., Int. Ed. Engl.* **1995**, *34*, 1209−1212.
(17) Johnston, A. G.; Leigh, D. A.; Nezhat, L.; Smart, J. P.; Deegan, M. D. *Angew. Chem., Int. Ed. Engl.* **1995**, *34*, 1212−1216.
(18) Kidd, T. J.; Leigh, D. A.; Wilson, A. J. *J. Am. Chem. Soc.* **1999**, *121*, 1599−1600.
(19) Lin, C. C.; Baliga, S. *J. Appl. Polym. Sci.* **1986**, *31*, 2483−2489.
(20) Medellin-Rodrigez, F. J.; Lopez-Guillen, R.; Waldo-Mendoza, M. A. *J. Appl. Polym. Sci.* **2000**, *75*, 78−86.
(21) Gross, S. M.; Roberts, G. W.; Kiserow, D. J.; DeSimone, J. M. *Macromolecules* **2000**, *33*, 40−45.
(22) van Bennekom, A. C. M.; Willemsen, P. A. A. T.; Gaymans, R. J. *Polymer* **1996**, *37*, 5447−5459.
(23) Weisskopf, K. *J. Polym. Sci., Polym. Chem. Ed.* **1988**, *26*, 1919−1935.
(24) Leigh, D. A.; Moody, K.; Smart, J. P.; Watson, K. J.; Slawin, A. M. Z. *Angew. Chem., Int. Ed. Engl.* **1996**, *35*, 306−310.
(25) Leigh, D A.; Murphy, A.; Smart, J. P.; Deleuze, M. S.; Zerbetto, F. *J. Am. Chem. Soc.* **1998**, *120*, 6458−6467.
(26) Pilati, F.; Toselli, M.; Messori, M.; Manzoni, C.; Turturro, A.; Gattiglia, E. G. *Polymer* **1997**, *38*, 4469−4476 and references therein.
(27) Kint, D. P. R.; Munoz-Guerra, S. *Polym. Int.* **2003**, *52*, 321−336 and references therein.
(28) Connor, D. M.; Allen, S. D.; Collard, D. M.; Liotta, C. L.; Schiraldi, D. A. *J. Appl. Polym. Sci.* **2001**, *81*, 1675−1682.
(29) Jog, J. P. *J. Macromol. Sci., Rev. Macromol. Chem.* **1995**, *C35*, 531−553.
(30) Fustin, C. A.; Bailly, C.; Clarkson, G. J.; Galow, T. H.; Leigh, D. A. *Macromolecules* **2004**, *37*, 66−70.
(31) James, N. R.; Ramesh, C.; Sivaram, S. *Macromol. Chem. Phys.* **2001**, *202*, 2267−2274.
(32) a) Rault, J.; Robelin, E.; Perez, G. *J. Macromol. Sci., Phys.* **1983**, *B22*, 577−589. (b) Robelin-Souffaché, E.; Rault, J. *Macromolecules* **1989**, *22*, 3581−3594.
(33) Haubruge, H. G.; Jonas, A. M.; Legras, R. *Macromolecules* **2004**, *37*, 126−134.
(34) Strobl, G. *The Physics of Polymers*; Springer-Verlag: Berlin, 1996.
(35) Ivanov, D. A.; Legras, R.; Jonas, A. M. *Macromolecules* **1999**, *32*, 1582−1592.

MA048575U